

---

# GENERALIZED STATISTICS: APPLICATIONS TO DATA INVERSE PROBLEMS WITH OUTLIER-RESISTANCE

---

**João V. T. de Lima**

Department of Theoretical and Experimental Physics  
Federal University of Rio Grande do Norte  
Natal, RN, 59078-970, Brazil.  
tomazvictor13@gmail.com

**Sérgio Luiz E. F. da Silva**

Seismic Inversion and Imaging Group  
Fluminense Federal University  
Niterói, RJ, 24210-346, Brazil  
sergioluizsilva@id.uff.br

**João M. de Araújo**

Department of Theoretical and Experimental Physics  
Federal University of Rio Grande do Norte  
Natal, RN, 59078-970, Brazil.  
joaomedeiros@fisica.ufrn.br

**Gilberto Corso**

Department of Biophysics and Pharmacology  
Federal University of Rio Grande do Norte  
Natal, RN, 59078-970, Brazil.  
gfcorso@gmail.com

**Gustavo Z. dos Santos Lima**

School of Science and Technology  
Federal University of Rio Grande do Norte  
Natal, RN, 59078-970, Brazil.  
guzampier76@gmail.com

## ABSTRACT

The conventional approach to data-driven inversion framework is based on Gaussian statistics that presents serious difficulties, especially in the presence of outliers in the measurements. In this work, we present maximum likelihood estimators associated with generalized Gaussian distributions in the context of Rényi, Tsallis and Kaniadakis statistics. In this regard, we analytically analyse the outlier-resistance of each proposal through the so-called influence function. In this way, we formulate inverse problems by constructing objective functions linked to the maximum likelihood estimators. To demonstrate the robustness of the generalized methodologies, we consider an important geophysical inverse problem with high noisy data with spikes. The results reveal that the best data inversion performance occurs when the entropic index from each generalized statistic is associated with objective functions proportional to the inverse of the error amplitude. We argue that in such a limit the three approaches are resistant to outliers and are also equivalent, which suggests a lower computational cost for the inversion process due to the reduction of numerical simulations to be performed and the fast convergence of the optimization process.

**Keywords** Inverse Problems · robust statistics · Generalized statistics · law of error · seismic inversion · influence function

## 1 Introduction

The estimation of physical model parameters from observed data is a frequent problem in many areas, such as in machine learning [1, 2], geophysics [3, 4], biology [5, 6], physics [7, 8], among others [9, 10, 11]. Such a task is solved through the so-called inverse problem, which consists of identifying physical parameters that can not be directly measured from the observations [12]. From a practical viewpoint, in the inverse problem, physical model parameters are estimated by matching the calculated data to the observed data by optimizing an objective function [13]. The objective function in the least-squares sense is widely used, which is based on the assumption that errors are independent and

identically distributed (*iid*) by a standard Gaussian probability distribution [12]. Although this approach is quite popular, the least-squares estimation is biased if the errors are non-Gaussian, violating the Gauss-Markov theorem [14, 15]. Indeed, just a few outliers are enough for the least-squares criterion to be inappropriate [16].

In this way, a lot of non-Gaussian criteria have been proposed to mitigate the inverse problem sensitivity to aberrant measurements (outliers). The most common criterion to deal with non-Gaussian errors is based on the  $L_1$ -norm of the difference between the calculated and the observed data, in which the errors are assumed to be *iid* according to a double exponential distribution (Laplace distribution) [17]. Although this approach is known for being outlier-insensitive, this criterion is singular in cases where the error is null (or close to zero). Thus, it is necessary to assume that the absolute error is greater than zero according to the machine precision used, which generates an indeterminacy problem from a computational point of view. To avoid the singularity of this approach, hybrid criteria which combine the least-squares distance with the least-absolute-values criterion ( $L_1$ -norm) have been proposed and successfully applied for parameter robust estimation [18, 19, 20]. However, hybrid approaches require the determination of a threshold parameter, which demands boring trial-and-error investigations, increasing the computational cost [21].

Indeed, objective functions based on heavy-tailed probability distributions, such as the Cauchy-Lorentz distribution [22] and the Student's  $t$ -distribution [23], have demonstrated robust properties for unbiased data inversion. However, both approaches assume a fixed probability distribution of errors, not adapting to the particularities of the model or data at hand. In this sense, objective functions based on generalized distributions are interesting because they might be adapted to the specificities of the erratic data by selecting an adequate free-parameter. In fact, several generalized approaches have been proposed to deal with erratic data [24, 25, 26, 27, 28]. Thus, generalized distributions based on the Rényi, Tsallis and Kaniadakis statistics have generated objective functions robust to erratic noise [29].

In this work, we consider deformed Gaussian distributions associated to generalized statistical mechanics in the sense of Rényi ( $\alpha$ -statistics) [30], Tsallis ( $q$ -statistics) [31] and Kaniadakis ( $\kappa$ -statistics) [32] to mitigate the undesirable effects of outliers on estimates of physical parameters. In particular, we place the objective functions based on  $\alpha$ -,  $q$ - and  $\kappa$ -generalizations in the broad context of the Gauss' law of error [33, 34, 35], see Refs. [29, 36, 37]. The three deformed Gaussian distributions mentioned above have already demonstrated robust properties in many applications [29, 36, 37, 38, 39, 40, 41, 42]. However, the entropic index associated with each of these approaches that make the inversion process more robust requires thorough investigation. In this regard, we analyse and compare the generalized objective functions from a statistical and numerical point of view in order to obtain the optimum value of the entropic index. The workflow of the experiments employed in this work is summarized in Fig. 1 in which it is represented a flowchart of an inverse problem. We call attention that in our framework, generalized statistics define the norm employed in the inversion problem solution.

We have organized this article as follows. In Section 2 we present a brief review on the solution of inverse problems using the maximum likelihood method in the conventional framework, as well as in the framework of Rényi, Tsallis and Kaniadakis. Moreover, in Section 2.4 we discuss the similarities among the generalized objective functions by considering a numerical test whose purpose is to estimate line model parameters; and finally, Section 3 is destined to apply the methodology presented in the article to address a classic geophysical problem that consists of estimating the acoustic impedance model using seismic data post-stack contaminated with spike noise.

## 2 A brief review of generalized statistical in inverse theory: Maximum likelihood methods

An inverse problem is formulated as an optimization task, in which an objective function describes how well the estimated model matches the measurements [12]. In this regard, the model parameters  $\mathbf{m}$  are obtained by solving the following linear system [12, 13]:

$$\mathbf{d}^{cal} = \mathbb{G}\mathbf{m}, \quad (1)$$

where  $\mathbf{d}^{cal}$  are the calculated data, in which  $\mathbb{G}$  represents the forward operator. It is worth emphasizing that inverse problems are ill-posed [43], which means that the solution of Eq. (1) is not unique. This is due, in general, to the fact that the observed data are band-limited and noisy. In this way, it is necessary to find methodologies capable to solve Eq. (1) for cases where the observed data,  $\mathbf{d}^{obs}$ , is corrupted by measurement errors, limitations in data acquisition, among other factors.

In the conventional approach, model parameters are estimated by maximizing the objective function is derived from the maximization of the Boltzmann-Gibbs-Shannon entropy (BGS):

$$\mathcal{S}_{BGS}[p] = - \sum_{i=1}^N p(x_i) \ln(p(x_i)), \quad (2)$$

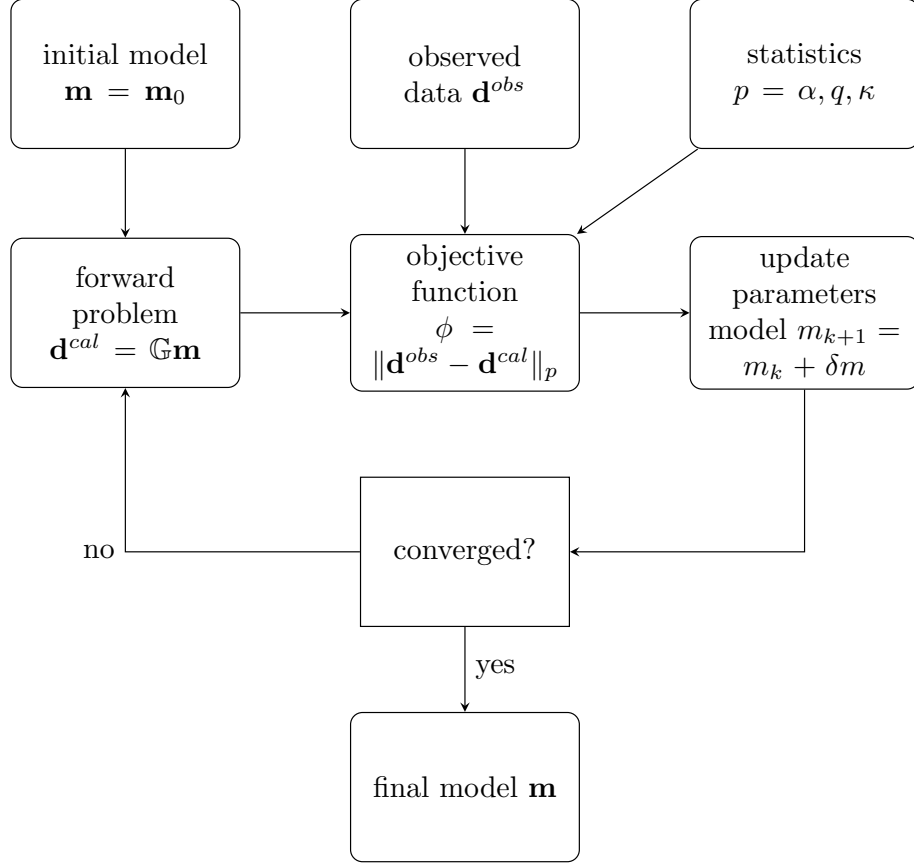


Figure 1: Workflow of the computational experiments.

subject to the following constraints:

$$\sum_{i=1}^N p(x_i) = 1 \quad (\text{normalization condition}), \quad (3)$$

$$\sum_{i=1}^N x_i^2 p(x_i) = 1 \quad (\text{unity variance}), \quad (4)$$

where  $p$  is a probability function and  $\mathbf{x} = \mathbf{d}^{obs} - \mathbf{d}^{cal} = \{x_1, x_2, \dots, x_N\}$  represents the difference between observed and calculated data. As well known in the literature, the probability distribution determined from the optimization of the BGS functional entropy subject to the constraints in Eqs. (3) and (4) corresponds to the standard Gaussian distribution (see, for instance, Section 2 of Ref. [40]):

$$p(x) = \frac{1}{\sqrt{2\pi}} \exp\left(-\frac{1}{2}x^2\right). \quad (5)$$

In other words, inverse problems, in the conventional framework, are solved from the premise that errors are independent and identically distributed (iid) according to a standard Gaussian likelihood function, which is formulated as the

following optimization problem:

$$\begin{aligned}\max_{\mathbf{m}} \mathcal{L}_G(\mathbf{m}) &= \prod_{i=1}^N p(x_i(\mathbf{m})) \\ &= \left(\frac{1}{\sqrt{2\pi}}\right)^N \exp\left(-\frac{1}{2} \sum_{i=1}^N x_i^2(\mathbf{m})\right).\end{aligned}\tag{6}$$

A likelihood function is a useful tool to estimate physical parameters from the empirical data. In practice, inverse problems based on the Gauss' law of error are formulated in a least-squares sense. To see this, we notice that maximizing the likelihood function in (6) is equivalent to minimizing the negative of the log-likelihood:

$$\begin{aligned}\min_{\mathbf{m}} \phi(\mathbf{m}) &= \frac{1}{2} \sum_{i=1}^N x_i^2(\mathbf{m}) \\ &= \frac{1}{2} \sum_{i=1}^N (d_i^{obs} - d_i^{cal}(\mathbf{m}))^2.\end{aligned}\tag{7}$$

However, it is worth emphasizing that in several problems the errors are non-Gaussian and, therefore, in such contexts the conventional approach becomes inefficient, especially in the presence of aberrant measures (outliers) [44].

As is already known, we obtain with Eq. (5) an adjustment to the data that is nothing more than a mean. For example, if we want to estimate  $\mathbb{G}m_k$ , where  $m_k$  is the  $k$ -th element of the parameter vector  $\mathbf{m}$ , from Eq. (5) we find the following stationary point

$$\begin{aligned}\frac{\partial p(m_k)}{\partial m_k} &= \frac{\partial}{\partial m_k} \frac{1}{\sqrt{2\pi}} \sum_{i=1}^N \exp\left(-\frac{1}{2}(d_i - \mathbb{G}m_k)^2\right) \\ &= 0 \\ \Rightarrow \mathbb{G}m_k &= \frac{1}{N} \sum_{i=1}^N d_i\end{aligned}\tag{8}$$

Therefore, if the observed data is contaminated with outliers, what we find using the conventional approach is the measurement of a mean, which in turn is strongly influenced by outliers and even more by a large amount of outliers.

For an objective function to admit a minimum, it must satisfy the condition

$$\sum_{i=1}^N c_i \mathcal{I}(x_i) = 0, \quad \text{with } \mathcal{I}(x) := \frac{\partial \phi(x)}{\partial m_k}\tag{9}$$

In Eq. (9)  $c_i$  are arbitrary constants and  $\mathcal{I}$  is the so-called influence function [40]. The influence function Eq. (9) informs us about the sensitivity of the objective function to outliers. In this sense, if  $\mathcal{I} \rightarrow \infty$  for a certain observed data  $d_i^{obs} \rightarrow \infty$ , the objective function is sensitive to outliers and, therefore, it is not a robust estimator. A robust estimate, however, will indicate  $\mathcal{I} \rightarrow 0$  for  $d_i^{obs} \rightarrow \infty$ . What we have in the conventional approach, however, is that the conventional objective function, Eq. (7), is linearly influenced by outliers, as in the following equation

$$\mathcal{I}(\mathbf{m}) = \sum_{i=1}^N x_i(\mathbf{m}) = - \sum_{i=1}^N \mathbb{G}^T (d_i^{obs} - \mathbb{G}\mathbf{m}).\tag{10}$$

The conventional theory of inverse problems, based on Gaussian statistics, failures with errors outside the Gaussian domain. In this sense, we look for alternatives to generalize Gaussian statistics in order to find more robust methods to deal with outliers.

## 2.1 Rényi's Framework

Based on information theory, A. Rényi [30, 45] introduced a general information entropy as a one-parameter generalization of the BGS entropy. Rényi entropy ( $\alpha$ -entropy) functional is expressed by:

$$\mathcal{S}_\alpha(p) = \frac{1}{1-\alpha} \ln \left( \sum_{i=1}^N p^\alpha(x_i) \right), \quad \alpha \geq 0,\tag{11}$$

where  $\alpha$  is the entropic index. Furthermore, the entropy in Eq. (11) shares many of the properties of the BGS entropy Eq. (2), such as: it is non-negative, it is additive, and it has an extreme for the case of equiprobability [30]. The fundamental difference between these two entropies resides in the non-conservation of the concavity, which is associated to the choice of index  $\alpha$ . Furthermore, Rényi's entropy recovers Shannon's entropy at the limit  $\alpha \rightarrow 1$ . Applications of Rényi entropy can be found in several fields [46, 47, 48].

Taking into account the constraints in Eqs. (3) and (4),  $\alpha$ -entropy is maximized by the  $\alpha$ -generalized Gaussian distribution,  $\alpha$ -Gaussian, which is expressed in the form [49, 50, 33]:

$$p_\alpha(x) = A_\alpha \left(1 - \frac{\alpha - 1}{3\alpha - 1} x^2\right)_+^{\frac{1}{\alpha-1}} \quad (12)$$

where  $[x]_+ = 0$  if  $x < 0$  and  $[x]_+ = x$ . In addition,  $A_\alpha$  is the normalizing constant:

$$A_\alpha = \begin{cases} \sqrt{\frac{1-\alpha}{[3\alpha-1]\pi}} \Gamma\left(\frac{1}{1-\alpha}\right) / \Gamma\left(\frac{1+\alpha}{2[1-\alpha]}\right), & \frac{1}{3} < \alpha < 1 \\ \sqrt{\frac{1-\alpha}{[3\alpha-1]\pi}} \Gamma\left(\frac{3\alpha-1}{2[1-\alpha]}\right) / \Gamma\left(\frac{\alpha}{\alpha-1}\right), & \alpha > 1 \end{cases} \quad (13)$$

with  $\Gamma(\cdot)$  representing the gamma function. At the limit  $\alpha \rightarrow 1$ , the ordinary Gaussian probability distribution Eq. (5) is recovered. Figure 2 shows some curves of the  $\alpha$ -Gaussian probability distribution. In particular, we note that at the limit  $\alpha \rightarrow 1/3$  the probability distribution approaches a strongly peaked function.

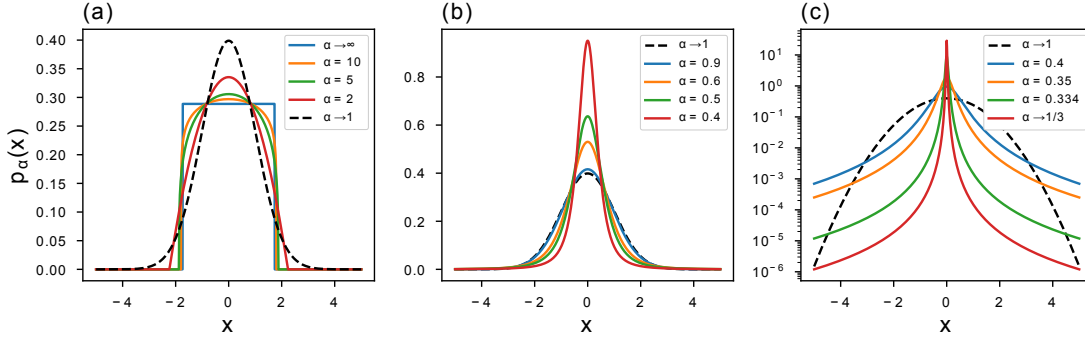


Figure 2:  $\alpha$ -Gaussian probability distribution. The black dashed line represents the conventional curves.

Following the same path discussed of the previous Section, that is, using the maximum likelihood method, we find a generalized objective function [29]:

$$\begin{aligned} \phi_\alpha(\mathbf{m}) &= \frac{1}{1-\alpha} \sum_{i=1}^N \ln \left(1 - \frac{\alpha-1}{3\alpha-1} x_i^2(\mathbf{m})\right)_+ \\ &= \|x_i\|_\alpha^2. \end{aligned} \quad (14)$$

This function will be called  $\alpha$ -objective function and at limit  $\alpha \rightarrow 1$  the conventional objective function, Eq. (7), is recovered. To investigate the behaviour of the  $\alpha$ -objective function regarding outliers we compute the influence function, as defined in Eq. (9), named  $\alpha$ -influence function:

$$\mathcal{I}_\alpha(\mathbf{m}) = \sum_{i=1}^N \frac{2x_i(\mathbf{m})}{(3\alpha-1 - (\alpha-1)x_i^2(\mathbf{m}))_+} \quad (15)$$

A couple of illustrative curves of the influence function are shown in Fig. 3, we draw our attention to the limit case  $\alpha \rightarrow 1/3$ . In this region the influence of the outliers is minimized:  $\mathcal{I}_\alpha(x_i \rightarrow \pm\infty) = 0$ , in contrast, the conventional objective function Eq. (7) is strongly influenced by outliers since  $\mathcal{I}(x_i \rightarrow \pm\infty) = \pm\infty$ .

## 2.2 Tsallis's Framework

Based on multifractals quantities and long-range interactions, C. Tsallis postulates an alternative form for the entropy to generalize the standard statistical mechanics [31]. Since then, a wide variety of applications have been performed based

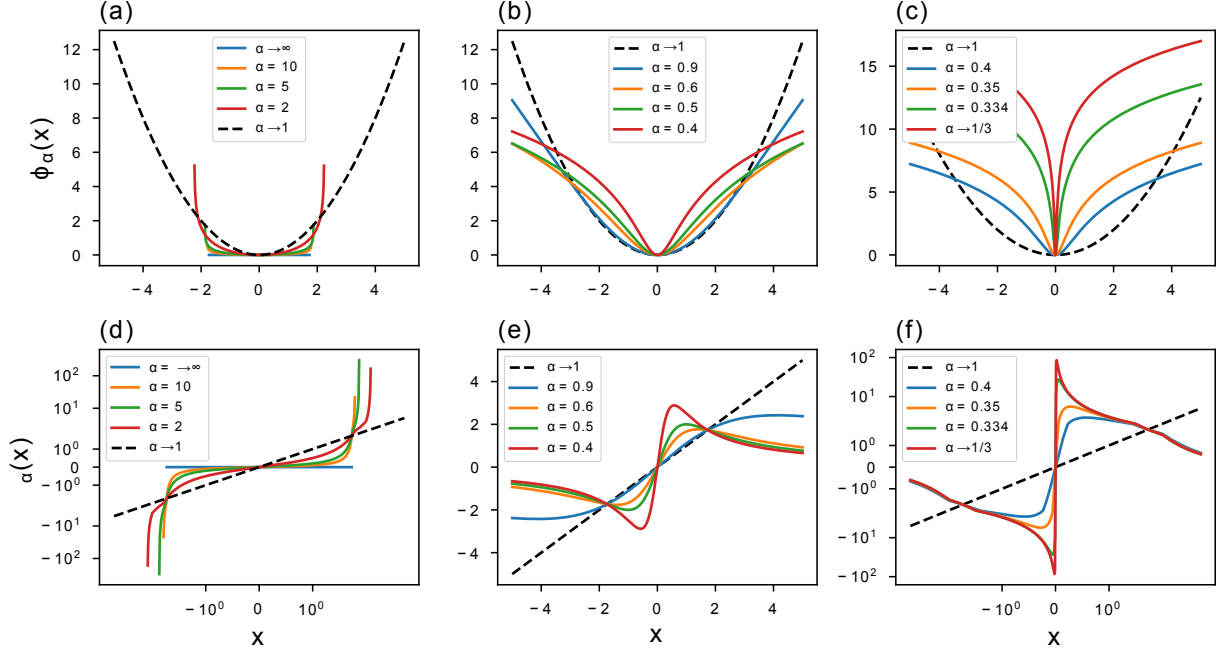


Figure 3: (a)-(c) objective functions and (d)-(f) influence functions generalized based on Rényi statistic. The black dashed line represents the conventional curves.

on Tsallis  $q$ -statistics [51, 52, 53, 54]. The Tsallis approach is based on the  $q$ -entropy, defined as follows:

$$S_q(p) = \frac{1}{q-1} \left( 1 - \sum_{i=1}^N p^q(x_i) \right), \quad (16)$$

where  $q \in \mathbb{R}$  is the entropic index (also known as nonextensive parameter). The choice of the entropic index  $q$  assigns new properties to the entropy functional, and in the limit case  $q \rightarrow 1$  it recovers the conventional BGS entropy.

By considering the maximum entropy principle for  $q$ -entropy, a  $q$ -generalization of Gauss' law of error was formulated in Ref. [55] assuming that the errors  $x$  follow an optimal probability distribution. In this regard, the optimal probability function is computed by maximizing the  $q$ -entropy constrained to the normalization condition, Eq. (3), and the  $q$ -variance [56, 57] given by:

$$\langle x \rangle_q^2 = \sum_{i=1}^N x_i^2 P_q(x_i), \quad \text{with } P_q(x_j) = \frac{p^q(x_j)}{\sum_{i=1}^N p^q(x_i)}, \quad (17)$$

in which  $P_q$  is the escort probability function [58, 59]. The probability distribution resulting from the aforementioned optimization problem is known by the  $q$ -Gaussian distribution:

$$p_q(x) = A_q \left( 1 + \frac{q-1}{3-q} x^2 \right)_+^{\frac{1}{1-q}} \quad (18)$$

where the normalization constant is given by [60]:

$$A_q = \begin{cases} \sqrt{\frac{1-q}{[3-q]\pi}} \Gamma\left(\frac{5-3q}{2[1-q]}\right) / \Gamma\left(\frac{2-q}{1-q}\right), & -\infty < q < 1 \\ \sqrt{\frac{q-1}{[3-q]\pi}} \Gamma\left(\frac{1}{q-1}\right) / \Gamma\left(\frac{3-q}{2[q-1]}\right), & 1 < q < 3 \end{cases} \quad (19)$$

A comparison between the conventional Eq. (2) and Tsallis approach Eq. (16) reveals that most probable events gain greater weight in the entropy calculation for the case in which  $q \neq 1$ . In this sense, the usual average is replaced by an average that depends on the choice of the index and so the higher the value of this index [61], the most likely events receive higher weights. Figure. 4 show illustrative curves of the  $q$ -Gaussian probability distribution. It is important to

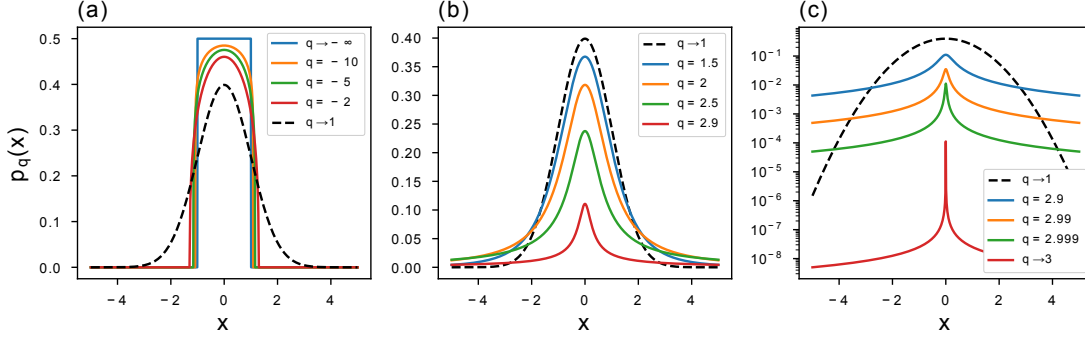


Figure 4:  $q$ -Gaussian probability distribution. The black dashed line represents the conventional curves.

note that at the limit  $q \rightarrow 3$  we have a behaviour that reminds us of the Rényi distribution in  $\alpha \rightarrow 1/3$ : at this limit both distributions display a peaked behaviour.

Applying the probabilistic maximum-likelihood method in the  $q$ -Gaussian distribution, we have the following objective function [36]

$$\begin{aligned} \phi_q(\mathbf{m}) &= \frac{1}{q-1} \sum_{i=1}^N \ln \left( 1 + \frac{q-1}{3-q} x_i^2(\mathbf{m}) \right)_+ \\ &= \|x_i\|_q^2 \end{aligned} \quad (20)$$

In order to check the influence of outliers for our objective function, we calculate the influence function [40]:

$$\mathcal{I}_q(\mathbf{m}) = \sum_{i=1}^N \frac{2x_i(\mathbf{m})}{(3-q + (q-1)x_i^2(\mathbf{m}))_+} \quad (21)$$

Equation (21) reveals that the Tsallis framework also shows a robust objective function that is resistant to outliers. Figure 5 displays a couple of influence function curves. At the limit  $x_i \rightarrow \pm\infty$ , the choice of index  $q < 1$  implies  $(3-q + (q-1)x_i^2)_+^{-1} \rightarrow \infty$  because the sum inside the brackets will always result in a negative quantity:  $\mathcal{I}_{q < 1}(\pm\infty) \rightarrow \infty$ . On the other hand, for  $q > 1$  the sum inside the brackets turns into a large positive number, leading to  $\mathcal{I}_{q > 1}(\pm\infty) \rightarrow 0$ .

### 2.3 Kaniadakis's Framework

G. Kaniadakis proposed a new way to calculate the entropy based on the principle of Kinetic Interaction [32, 62]. This new  $\kappa$ -entropy that generalizes the BGS statistics is given by:

$$\mathcal{S}_\kappa(p) = -\frac{1}{2\kappa} \sum_{i=1}^N \left( p^{1+\kappa}(x_i) - p^{1-\kappa}(x_i) \right) \quad (22)$$

Kaniadakis statistics has been applied in different contexts [63, 64, 65]. The conventional entropy (BGS) is recovered in the limit of the entropic index  $\kappa \rightarrow 0$ . Kaniadakis' framework not only includes conventional BGS statistics, but it is related to other statistics, such as the famous quantum statistics of Fermi-Dirac and Bose-Einstein, as well as the Tsallis [32, 66].

Based on the  $\kappa$ -Gaussian statistic, the reference [67] presents an error law that can be applied to a variety of problems and that, because it has a heavy tails distribution, it is able to satisfactorily work with outliers. The  $\kappa$ -Gaussian distribution is given by

$$p_\kappa(x) = \frac{1}{A_\kappa} \left( \sqrt{1 + \kappa^2 \beta_\kappa^2 x^4} - \kappa \beta_\kappa x^2 \right)^{1/\kappa} \quad (23)$$

where  $A_\kappa$  is the normalization constant given by

$$A_\kappa = \left( 1 + \frac{|\kappa|}{2} \right) \sqrt{\frac{2|\kappa|\beta_\kappa}{\pi}} \frac{\Gamma(1/|2\kappa| + 1/4)}{\Gamma(1/|2\kappa| - 1/4)} \quad (24)$$

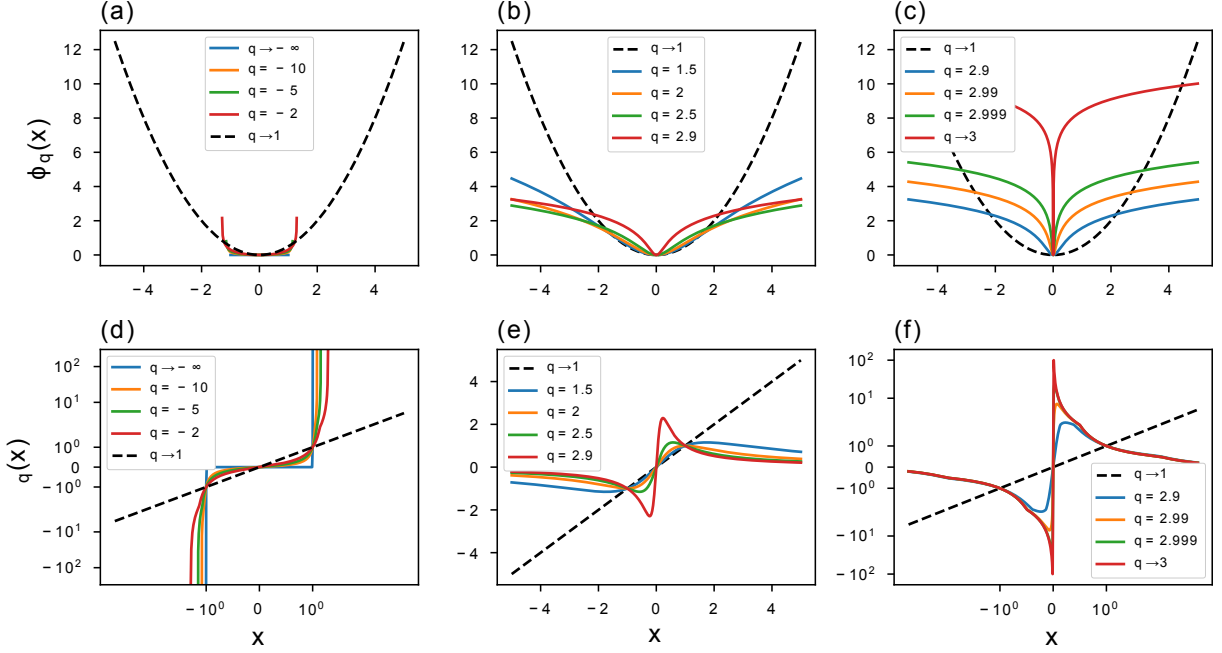


Figure 5: (a)-(c) objective functions and (d)-(f) generalized influence functions based on Tsallis statistic. The black dashed line represents the conventional curves.

and  $\beta_\kappa > 0$  depends on the  $\kappa$  index and is given by:

$$\beta_\kappa = \frac{1 + |\kappa|/2}{|2\kappa| (2 + 3|\kappa|)} \times \frac{\Gamma(1/|2\kappa| - 3/4) \Gamma(1/|2\kappa| + 3/4)}{\Gamma(1/|2\kappa| + 1/4) \Gamma(1/|2\kappa| - 1/4)} \quad (25)$$

Some curves of the  $\kappa$ -Gaussian distribution are shown in Fig. 6. We notice that the distribution has heavy tails when choosing  $\kappa \rightarrow 2/3$  and at this limit, as well as in the  $\alpha$ -Gaussian and  $q$ -Gaussian distributions, the distribution shows a peaked behaviour that resembles the Dirac delta distribution.

In this scenario, the inverse problem is therefore formulated as the problem of optimizing the  $\kappa$ -objective function that derives from the principle of maximum likelihood

$$\begin{aligned} \phi_\kappa(\mathbf{m}) &= -\frac{1}{\kappa} \sum_{i=1}^N \ln \left( \sqrt{1 + \kappa^2 \beta_\kappa^2 x_i^4(\mathbf{m})} - \kappa \beta_\kappa x_i^2(\mathbf{m}) \right) \\ &= \|x_i\|_\kappa^2 \end{aligned} \quad (26)$$

and the analysis of the robustness of this objective function can be performed by the  $\kappa$ -influence function, which is given by:

$$\mathcal{I}_\kappa(\mathbf{m}) = \sum_{i=1}^N \frac{2\beta_\kappa x_i(\mathbf{m})}{\sqrt{1 + \kappa^2 \beta_\kappa^2 x_i^4(\mathbf{m})}} \quad (27)$$

The curves of the  $\kappa$ -objective and  $\kappa$ -influence functions are shown in Fig. 7. In Fig. 7(c)-(d) we notice that as we increase the value of index  $\kappa$  the influence of distant values of  $x = 0$  decreases. In particular, at the limit  $\kappa \rightarrow 2/3$  we observe the curve that indicates less influence for  $x \rightarrow \pm\infty$  measurements. Looking at Eq. (27) we noticed that for  $x_i \rightarrow \pm\infty$  we have  $\mathcal{I}_\kappa(x_i \rightarrow \pm\infty) = 0$ .



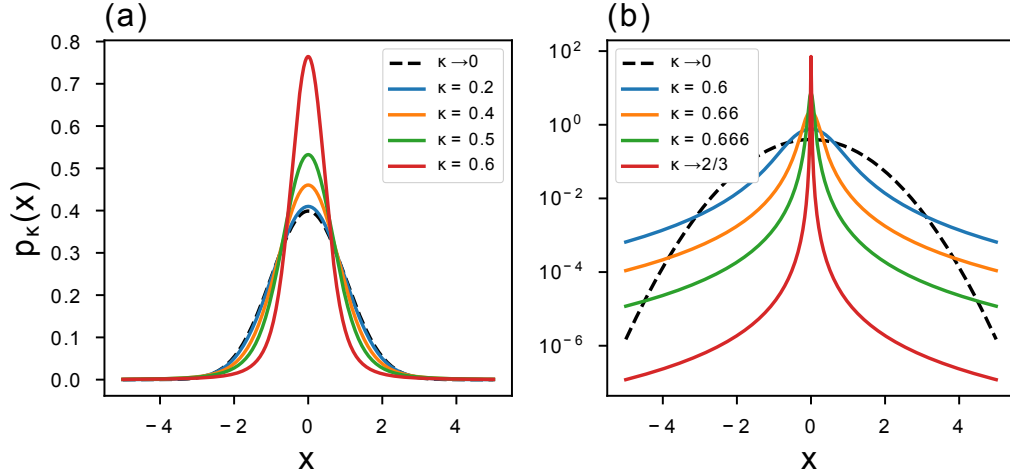


Figure 6:  $\kappa$ -Gaussian probability distribution. The black dashed line represents the conventional curves.

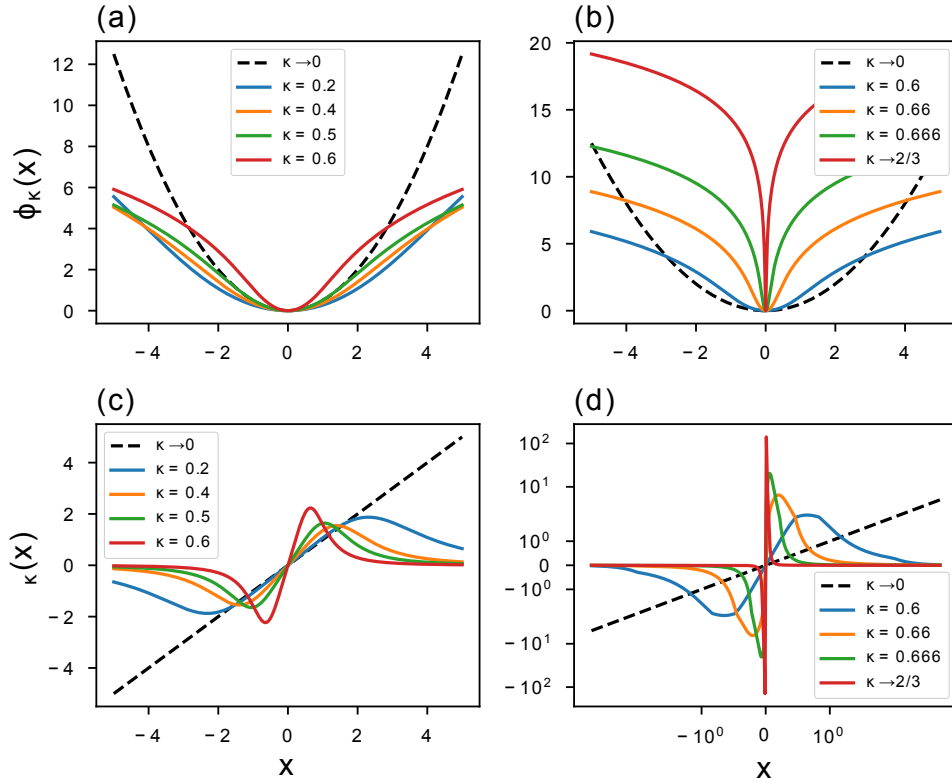


Figure 7: (a)-(b) objective functions and (c)-(d) generalized influence functions based on Kaniadakis statistic. The black dashed line represents the conventional curves.

## 2.4 Comparing the performance of objective functions

In this section, we present a simple numerical experiment in order to quantitatively analyse the robustness of objective functions based on generalized statistics. The experiment consists of estimating the coefficients  $\mathbf{m} = \{m_1, m_2\}$  of a linear polynomial,  $d^{cal} = m_1x + m_2$ , from observed data  $\mathbf{d}^{obs}$  contaminated by outliers. In this regard, we consider

the independent variable  $x \in \mathbb{R}^{50}$  within the range  $[-1, 1]$  to generate 50 numbers obeying a linear polynomial with coefficients  $m_1 = 1$  and  $m_2 = 2$ . Then we contaminate the numbers generated with a Gaussian distribution with zero-mean and standard-deviation  $\sigma^2 = 0.2$ . In addition, the variable  $d^{obs}$  is contaminated with outliers in region  $0.4 \leq x < 0.9$ , of  $d^{obs}$ , the outliers are given by  $d_i^{obs} = 10f$  where  $f$  is a Gaussian random variable.

Conventionally, this problem is treated by minimizing the square of the residuals based on Gaussian statistics [13, 68]. However, as discussed in Eq. (8), the Gaussian estimate is not appropriate to solve problems with discrepant values. In this sense, we propose to estimate the coefficients  $\mathbf{m}$  using the objective functions of Rényi (Eq. (14)), Tsallis (Eq. (20)) and Kaniadakis (Eq. (26)). The values of the entropic index were used between  $1 \leq \alpha \leq 0.3334$ ,  $1 \leq q \leq 2.9999$  and  $0 \leq \kappa \leq 0.6666$ . Inside each interval, 200 uniform spaced values were taken.

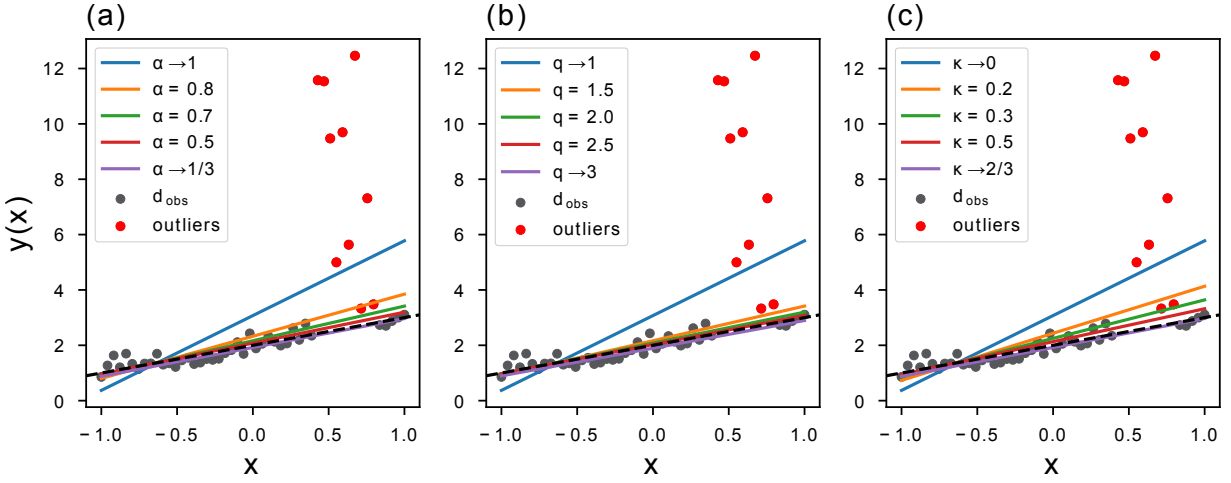


Figure 8: Fit of the estimated lines using the objective functions of (a) Rényi, (b) Tsallis and (c) Kaniadakis. The dashed line indicates an ideal line, and the points highlighted in red indicate the inserted outliers.

The calculated models,  $\mathbf{m}^{cal} = \{m_1^{cal}, m_2^{cal}\}$ , are compared with the ideal model  $\mathbf{m} = \{1, 2\}$  to find for each objective function the best entropic index that achieve an optimal fitting. Figure 9 correlates the estimated values of the intercept,  $\Delta m_1 = m_1^{cal} - 1$ , and the slope,  $\Delta m_2 = m_2^{cal} - 2$ , with the employed entropic index. We can see that as we move away from the Gaussian limit, we find a better fit.

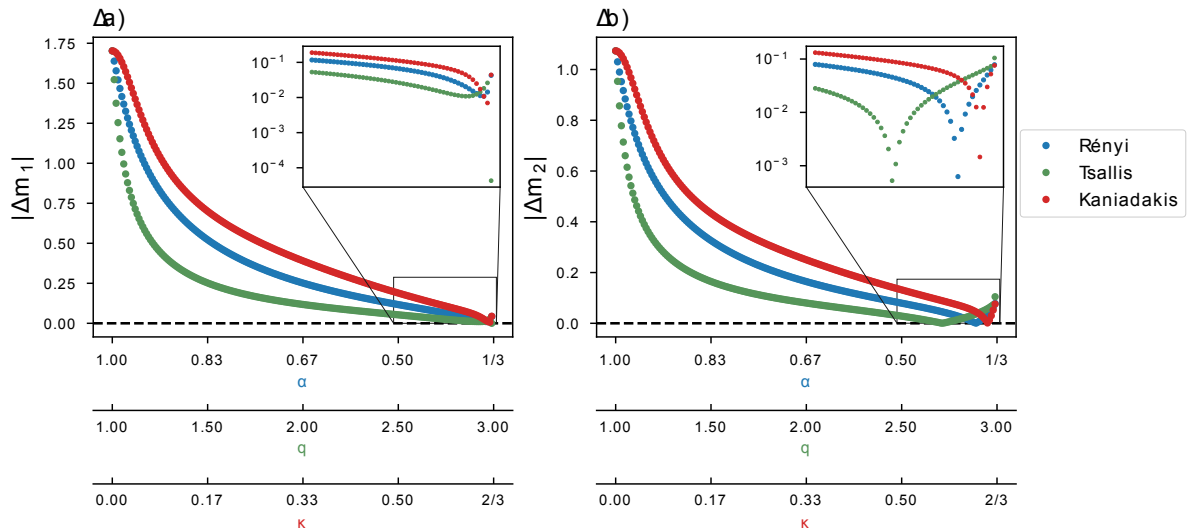


Figure 9: Relation between estimated parameters and entropic indexes. The zoom in window in (a) and (b) emphasizes the regions  $0.5 \leq \alpha < 1/3$ ,  $2.5 \leq q < 3$  and  $0.5 \leq \kappa < 2/3$

We compared the lines obtained with the estimated parameters, calculating the Mean Absolute Error,  $MAE = \sum_i |d_i(\mathbf{m}^{cal}) - d_i(\mathbf{m})| / N$ , between the calculated line,  $d(\mathbf{m}^{cal})$ , and the ideal line,  $d(\mathbf{m})$ . The obtained results are:  $MAE_\alpha = 0.0136$  with index  $\alpha = 0.3635$ ;  $MAE_q = 0.0134$  with  $q = 2.7587$  and  $MAE_\kappa = 0.0127$  with  $\kappa = 0.6532$ . The  $MAE$  represents the average deviation between predicted and reference values, and the best result is achieved for  $MAE$  close to zero. In contrast, the  $MAE$  calculated with the conventional objective function was 1.2000.

With this test, we observe that the results improve as we move away from the Gaussian limit. In particular, we notice that in Fig. 9 the green curve corresponding to the Tsallis result shows the steepest decrease after the Gaussian limit ( $q = 1$ ), while the red curve (Kaniadakis) presents a curve that slowly decreases after the Gaussian limit.

An analysis of the influence functions, Eqs. (15), (21) and (27), reveals that they are zero for  $x_i \rightarrow \pm\infty$ , regardless of the choice of entropic indexes (obviously, disregarding the conventional limit). In addition, we notice that in the limits  $\alpha \rightarrow 1/3$ ,  $q \rightarrow 3$  and  $\kappa \rightarrow 2/3$  the influence functions are merely a function that depends on the inverse of  $x_i$ . Thus, the three objective functions, Eqs. (14), (20) and (26), are resistant to outliers and have an entropic index limit in which they are equivalent.

### 3 Numerical experiments

In this section, we present numerical experiments to demonstrate the outlier-resistance of the data-inversion method based on generalized statistics by considering an important problem that comes from geophysics, which is an important process to obtain estimates of subsurface properties. In particular, we address a problem of seismic inversion known as Post-Stack Inversion (PSI) [69]. The goal of PSI is to estimate, from the observation of the seismic data, the acoustic impedance, which is a property of the rock defined as the product of the density of the rock and the speed of the acoustic wave in the subsurface [70].

The forward problem is formulated through the following relationship:  $\mathbf{d}^{cal} = \mathbb{W}\mathbb{D}\mathbf{m}$ . Here,  $\mathbf{d}^{cal}$  represents the seismic data calculated by the parameters  $\mathbf{m} = \ln(\mathbf{Z})$  which is used to estimate the acoustic impedance  $\mathbf{Z}$ . The operators  $\mathbb{W}$  and  $\mathbb{D}$  are described by [71]:

$$\mathbb{W} = \begin{bmatrix} \omega_1 & 0 & \dots & 0 \\ \vdots & \omega_1 & \vdots & 0 \\ \omega_n & \vdots & \ddots & 0 \\ 0 & \omega_n & \vdots & \omega_1 \\ \vdots & \vdots & \ddots & \vdots \\ 0 & \dots & \dots & \omega_n \end{bmatrix}, \quad \mathbb{D} = \frac{1}{2} \begin{bmatrix} -1 & 1 & 0 & \dots & 0 \\ 0 & -1 & 1 & \dots & 0 \\ \vdots & \vdots & \ddots & \ddots & 0 \\ 0 & \dots & \dots & -1 & 1 \end{bmatrix}. \quad (28)$$

Where  $\mathbb{W}$  is the wavelet operator, which computes the convolution between the seismic signal and  $\mathbb{D}\mathbf{m}$ . Finally,  $\mathbb{D}$  represents the first order derivative operator. In addition, we can group these two matrices into a single operator  $\mathbb{G} = \mathbb{W}\mathbb{D}$ . In this way, we compute the residuals between the observed data and the calculated data  $\mathbf{x} = \mathbf{d}^{obs} - \mathbb{G}\mathbf{m}$ .

To analyse the outlier-resistance of the objective functions presented in Section 2, we consider a portion of the synthetic geological Marmousi2 [72, 73] model as a benchmark (true model). In particular, we take into account the acoustic impedance model that consists of 5 km of depth and 1 km of distance as depicted in Fig. 10. The seismic source used was a Ricker wavelet [74, 75] with the peak frequency  $\nu_p = 55 \text{ Hz}$  (the most energetic frequency).

We test the robustness of the generalized objective functions using seismic data contaminated with white Gaussian noise with low intensity (taking a signal-to-noise ratio equal to 80 dB in all scenarios) and spikes (outliers) with different intensities, as shown in Fig. 11. The spikes were added by randomly choosing positions in the seismic data and adding peaks with intensities between  $5f$  and  $15f$  times the original amplitude, where  $f$  is a Gaussian random variable. We considered 161 noise scenarios, where the difference is in the percentages of samples contaminated by the outliers. In this regard, the number of samples were chosen from 0% to 80% of the data samples, with steps of 0.5%.

For each spiky-noise scenario, we carried out data-inversions employing the  $\alpha$ -,  $q$ - and  $\kappa$ -objective functions, Eqs. (14), (20) and (26), respectively with  $1/3 < \alpha \leq 1$ ,  $1 \leq q < 3$  and  $0 \leq \kappa \leq 2/3$  using 200 values for each of these parameters with uniform spacing between intervals. In total, for each objective function, we get 32.000 results. To minimize the objective functions, we employ the conjugate gradient method [76, 77], defining a maximum of 10 iterations and a tolerance error  $\epsilon = 10^{-12}$ .

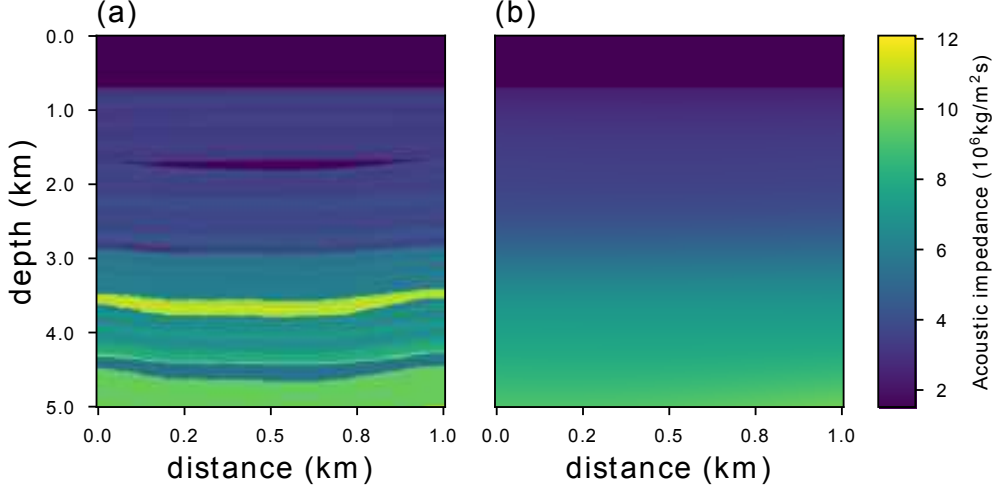


Figure 10: The geophysical model employed to illustrate the inversion methodology. In (a) the synthetic acoustic impedance model called Marmousi2. In (b) we show the initial model employed in the inversion methodology.

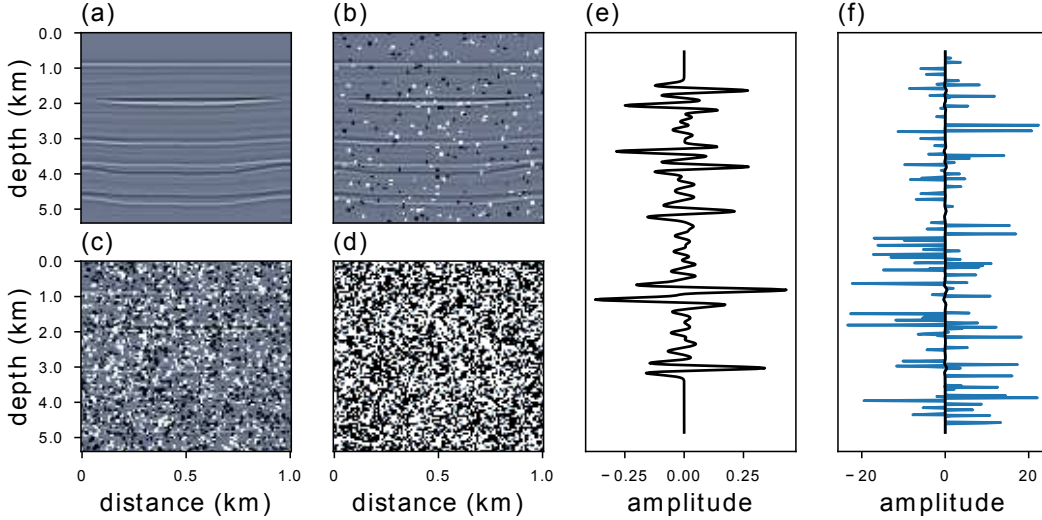


Figure 11: The noiseless seismic data in (a). The same data contaminated with white-noise (signal-to-noise ratio  $SNR = 80$ ) and spike noise with (b) 0.5%, (c) 5%, and (d) 80%. The black line in panels (e) represents a single seismic trace from the middle of panel (a). The same trace contaminated by noise is represented in (f) spikes (25%).

We consider the Pearson's correlation coefficient [78] as the statistical metric to compare the PSI results, which is defined as:

$$R = \frac{\sum_{n=1}^N \Delta_n^{true} \Delta_n^{rec}}{\sqrt{\sum_{n=1}^N (\Delta_n^{true})^2} \sqrt{\sum_{n=1}^N (\Delta_n^{rec})^2}} \quad (29)$$

where  $\Delta_n^{true} = Z_n^{true} - \mu^{true}$  and  $\Delta_n^{rec} = Z_n^{rec} - \mu^{rec}$  is the difference between the true and recovered acoustic impedance models,  $Z$ , and their respective averages,  $\mu$ . The coefficient  $R$  assume values between  $-1$  and  $+1$ . The case of  $R$  close to zero implies in absence of correlation. The correlation being strong when it approaches one.

Figures 12 and 13 show the recovered acoustic impedance for conventional and generalized objective functions. We notice that the PSI results obtained with the conventional objective function are severely affected by the presence of outliers. On the other hand, at the limits  $\alpha \rightarrow 1/3$ ,  $q \rightarrow 3$  and  $\kappa \rightarrow 2/3$  the influence of spikes are minimized, and good estimates are obtained.

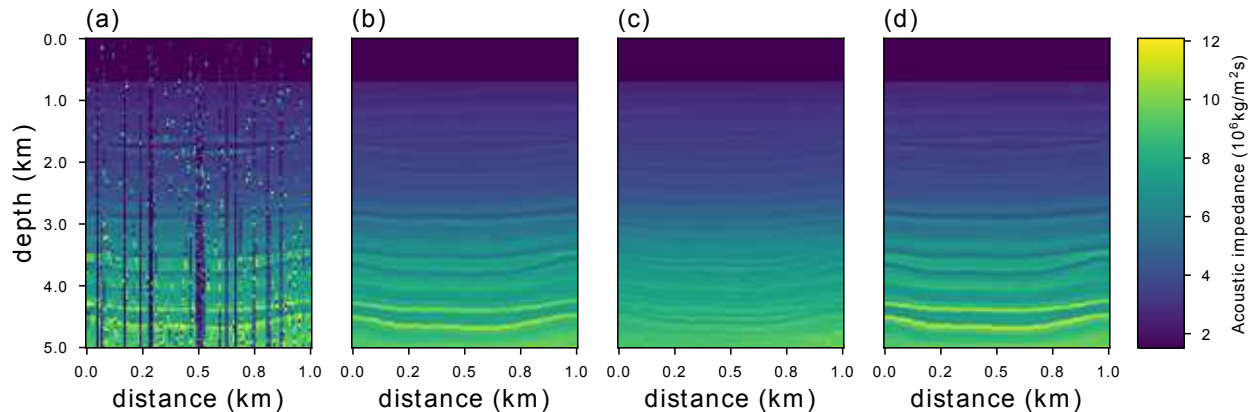


Figure 12: Acoustic impedance model recovered for an observed data contaminated with white noise (SNR = 80) and spike noise (0.5%) using objective function (a) conventional (b) Rényi with  $\alpha = 0.3334$ ; (c) Tsallis with  $q = 2.9999$ ; and (d) Kaniadakis with  $\kappa = 0.6666$

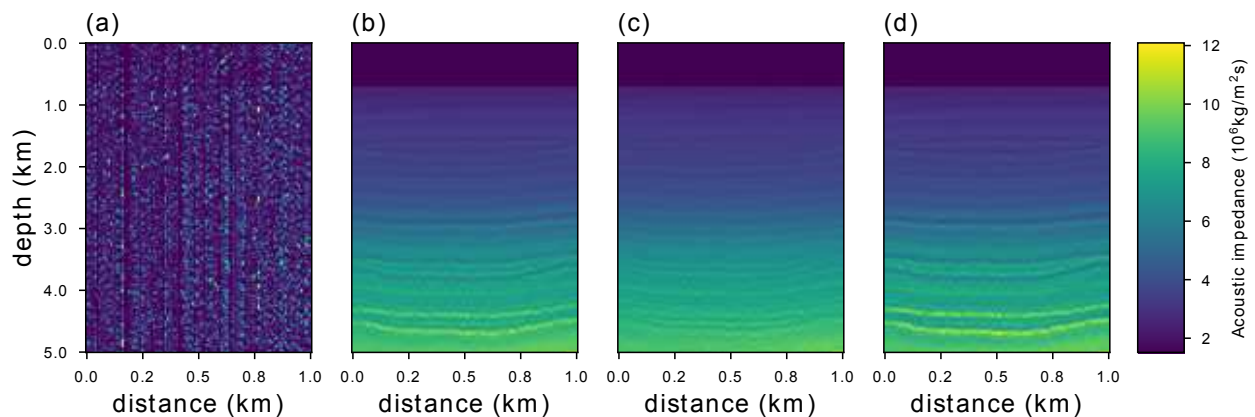


Figure 13: Acoustic impedance model recovered for an observed data contaminated with white noise (SNR = 80) and spike noise (80%) using objective function (a) conventional (b) Rényi with  $\alpha = 0.3334$ ; (c) Tsallis with  $q = 2.9999$ ; and (d) Kaniadakis with  $\kappa = 0.6666$

We summarize the PSI results for all numerical simulations performed in the present work in Fig. 14. In this figure, we remark that the objective functions present satisfactory results in  $\alpha \rightarrow 1/3$ ,  $q \rightarrow 3$  and  $\kappa \rightarrow 2/3$  limit cases, as predicted by the numerical experiment presented in Section 2.4. Indeed, in these limit cases, the generalized objective functions are robust tools capable of mitigate the influence of outliers, which leads to good results even for high spike contamination. In addition, it should be noted that the PSI results related with the reddish regions of the heatmap in Fig. 14 show a strong correlation regardless of the contamination rate employed.

## 4 Conclusions

In this work we explore robust methods based on the Rényi, Tsallis and Kaniadakis generalized statistics. Since the solution of the data-inversion strongly depends on the employed objective function, the generalized objective functions are indeed valuable for this purpose. In fact, given a proper choice of the entropic index, it is possible to get a robust objective function that handles errors that do not obey the Gaussian statistics.

In particular, we investigate a special example of non-Gaussian errors: outliers. In this scenario, we seek to answer some basic questions: (i) what is the most appropriate choice for entropic indexes? (ii) Which of the proposed methods is more resistant to outliers? For the first question, we find that there is a limit for every method in which the objective functions are able to ignore aberrant values without compromising the results. In addition, we note that the properties of the  $\alpha$ -,  $q$ - and  $\kappa$ -generalized distributions and the respective objective functions have similar characteristics at the limit:  $(\alpha, q, \kappa) \rightarrow (1/3, 3, 2/3)$ .

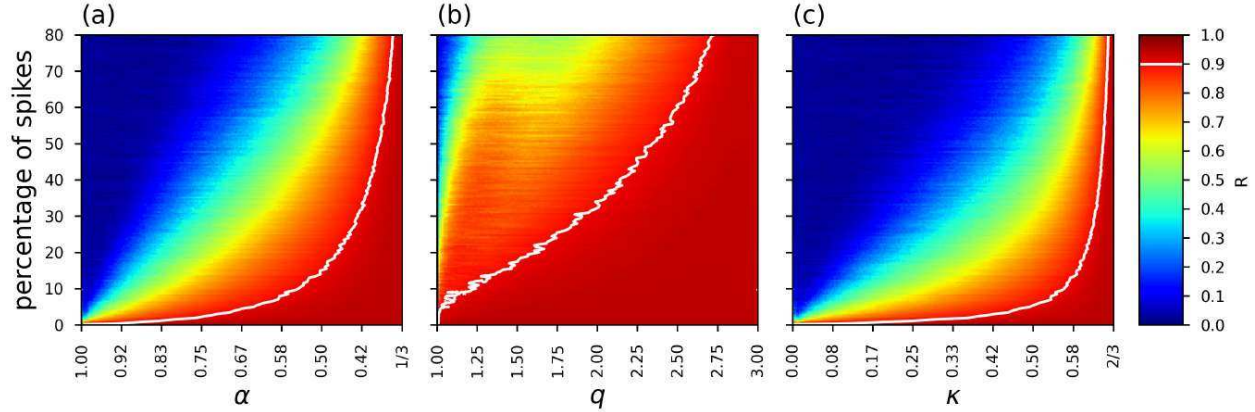


Figure 14: Heatmap representing the correlation between synthetic and recovered impedance models for the objective functions: (a) Rényi, (b) Tsallis and (c) Kaniadakis. The white markings indicate points such that  $R = 0.9$  (strong correlation).

To conclude, it is worth emphasizing that although these methodologies have been successfully employed in geophysical applications, our proposals are easily adaptable to a wide variety of parameter estimation problems. In this regard, we hope that the methodologies proposed in this work are of great value for the modelling of complex systems with numerous unknown variables, as the generalized objective functions are able to reduce the computational cost by accelerating the convergence of the process of optimization, as shown by analysing the influence function.

## Acknowledgements

J.V.T. de Lima, J.M. de Araújo, G. Corso and G.Z. dos Santos Lima gratefully acknowledge support from *Petrobras* through the project "*Statistical physics inversion for multi-parameters in reservoir characterisation*" at Federal University of Rio Grande do Norte. J.M. de Araújo thanks *Conselho Nacional de Desenvolvimento Científico e Tecnológico (CNPq)* for his productivity fellowship (grant no. 313431/2018-3). G. Corso acknowledges *CNPq* for support through productivity fellowship (grant no. 307907/2019-8).

## Declarations

### Conflicts of interest

The authors declare that they have no conflict of interest.

### Author contribution statement

All authors contributed equally to this work.

## References

- [1] M. Raissi, P. Perdikaris, and G. E. Karniadakis. Physics-informed neural networks: A deep learning framework for solving forward and inverse problems involving nonlinear partial differential equations. *J. Comput. Phys.*, 378:686–707, 2019.
- [2] John Harlim, Shixiao W. Jiang, Senwei Liang, and Haizhao Yang. Machine learning for prediction with missing dynamics. *J. Comput. Phys.*, 428:109922, 2021.
- [3] S. L. E. F. da Silva, J. Julià, and F. H. R. Bezerra. Deviatoric moment tensor solutions from spectral amplitudes in surface network recordings: Case study in São Caetano, Pernambuco, Brazil. *Bull. Seism. Soc. Am.*, 107:1495–1511, 2017.

- [4] Sérgio Luiz E. F. da Silva, Pedro T. C. Carvalho, Carlos A. N. da Costa, João M. de Araújo, and Gilberto Corso. An objective function for full-waveform inversion based on frequency-dependent offset-preconditioning. *PLoS One*, 15:e0240999, 2020.
- [5] Heinz W Engl, Christoph Flamm, Philipp Kügler, James Lu, Stefan Müller, and Peter Schuster. Inverse problems in systems biology. *Inverse Probl.*, 25:123014, 2009.
- [6] Gilles Clermont and Sven Zenker. The inverse problem in mathematical biology. *Math. Biosci.*, 260:11–15, 2015.
- [7] Yuming Ba, Lijian Jiang, and Na Ou. A two-stage ensemble Kalman filter based on multiscale model reduction for inverse problems in time fractional diffusion-wave equations. *J. Comput. Phys*, 374:300–330, 2018.
- [8] M. Razavy. *An Introduction to Inverse Problems in Physics*. World Scientific Publishing Company, New Jersey, 2012.
- [9] G. Kuramshina. *Inverse Problems of Molecular Spectra Data Processing*. In: Wang Y., Yang C., Yagola A.G. (eds) Optimization and Regularization for Computational Inverse Problems and Applications. Springer, Berlin, Heidelberg, 2010.
- [10] F. W. de Freitas Silva, S. L. E. F. da Silva, M. V. C. Henriques, and G. Corso. Using fish lateral line sensing to improve seismic acquisition and processing. *PLoS ONE*, 14:e0213847, 2019.
- [11] Gennadij Heidel, Venera Khoromskaia, Boris N. Khoromskij, and Volker Schulz. Tensor product method for fast solution of optimal control problems with fractional multidimensional Laplacian in constraints. *J. Comput. Phys*, 424:109865, 2021.
- [12] Albert Tarantola. *Inverse Problem Theory and Methods for Model Parameter Estimation*. SIAM, 2005.
- [13] William Menke. *Geophysical Data Analysis: Discrete Inverse Theory*. Academic Press, 2012.
- [14] M. Kendall and A. Stuart. *The Advanced Theory of Statistics: Inference and Relationship*. Hodder Arnold, London, 1979.
- [15] Richard E. Thomson and William J. Emery. Chapter 3 - Statistical Methods and Error Handling. In Richard E. Thomson and William J. Emery, editors, *Data Analysis Methods in Physical Oceanography (Third Edition)*, pages 219–311. Elsevier, Boston, third edition edition, 2014.
- [16] John A Scales and Adam Gersztenkorn. Robust methods in inverse theory. *Inverse Probl.*, 4:1071–1091, 1988.
- [17] A. Tarantola. *Inverse problem theory: Methods for data fitting and model parameter estimation*. Elsevier Scientific Publ. Co., 1987.
- [18] Peter J Huber et al. Robust Regression: Asymptotics, Conjectures and Monte Carlo. *Ann. Stat.*, 1(5):799–821, 1973.
- [19] Antoine Guitton and William W. Symes. Robust inversion of seismic data using the Huber norm. *Geophysics*, 68(4):1310–1319, 2003.
- [20] Kenneth P. Bube and Robert T. Langan. Hybrid  $l1/l2$  minimization with applications to tomography. *Geophysics*, 62:1183–1195, 1997.
- [21] R. Brossier, S. Operto, and J. Virieux. Which data residual norm for robust elastic frequency-domain full waveform inversion? *Geophysics*, 75(3):R37–R46, 2010.
- [22] P. Zhou, Y. Lv, H. Wang, and T. Chai. Data-driven robust RVFLNs modeling of a blast furnace iron-making process using cauchy distribution weighted M-estimation. *IEEE Trans. Ind. Electron.*, 64:7141–7151, 2017.
- [23] A. Ubaidillah, K. A. Notodiputro, A. Kurnia, A. Fitrianto, and I. W. Mangku. A robustness study of student-t distributions in regression models with application to infant birth weight data in Indonesia. *IOP Conf. Ser.: Earth Environ. Sci.*, 58:012013, 2017.
- [24] Zhiyong Li\*, Zhining Liu, Chengyun Song, Guangmin Hu, and Jiashu Zhang. *Generalized Gaussian distribution based adaptive mixed-norm inversion for non-Gaussian noise*, pages 3926–3930. Society of Exploration Geophysicists, 2015.
- [25] Fernanda Carozzi and Mauricio D. Sacchi. *Making seismic reconstruction more robust via a generalized loss function*, pages 3149–3153. Society of Exploration Geophysicists, 2020.
- [26] Sérgio Luiz E. F. da Silva and G. Kaniadakis. Robust parameter estimation based on the generalized log-likelihood in the context of Sharma-Taneja-Mittal measure. *Phys. Rev. E*, 104:024107, 2021.
- [27] Suzane A. Silva, Sérgio Luiz E. F. da Silva, Renato F. de Souza, Andre A. Marinho, João M. de Araújo, and Claudionor G. Bezerra. Improving seismic inversion robustness via deformed Jackson Gaussian. *Entropy*, 23:1081, 2021.

- [28] Sérgio L. E. F. da Silva, J. M. de Araújo, and G. Corso. Full-waveform inversion based on  $q$ -Laplace distribution. *Pure Appl. Geophys.*, 178:3415, 2021.
- [29] Sérgio Luiz Eduardo Ferreira da Silva, Gustavo Zampier dos Santos Lima, João Medeiros de Araújo, and Gilberto Corso. Extensive and nonextensive statistics in seismic inversion. *Physica A: Statistical Mechanics and its Applications*, 563:125496, 2021.
- [30] A. Rényi. On the foundations of information theory. *Rev. Inst. Int. Stat.*, 33(1):1–14, 1965.
- [31] C. Tsallis. Possible generalization of Boltzmann-Gibbs statistics. *J. Stat. Phys.*, 52:479–487, 1988.
- [32] G Kaniadakis. Non-linear kinetics underlying generalized statistics. *Physica A*, 296(3-4):405–425, 2001.
- [33] Hisa-Aki Tanaka, Masaki Nakagawa, and Yasutada Oohama. A direct link between Rényi-Tsallis entropy and hölder’s inequality—yet another proof of Rényi-Tsallis entropy maximization. *Entropy*, 21(6):549, May 2019.
- [34] H. Suyari and M. Tsukada. Law of error in tsallis statistics. *IEEE Trans. Inf. Theory*, 51(2):753–757, 2005.
- [35] Tatsuaki Wada and Hiroki Suyari.  $\kappa$ -generalization of Gauss’ law of error. *Phys. Lett. A*, 348(3):89–93, 2006.
- [36] Sérgio Luiz Eduardo Ferreira da Silva, Carlos AN da Costa, Pedro Tiago C Carvalho, João Medeiros de Araújo, Liacir dos Santos Lucena, and Gilberto Corso. Robust full-waveform inversion using  $q$ -statistics. *Physica A*, 548:124473, 2020.
- [37] Sérgio Luiz E. F. da Silva, Pedro Tiago C. Carvalho, J. M. de Araújo, and Gilberto Corso. Full-waveform inversion based on Kaniadakis statistics. *Phys. Rev. E*, 101:053311, 2020.
- [38] I. P. de Lima, S. L. E. F. da Silva, G. Corso, and J. M. de Araújo. Tsallis entropy, likelihood, and the robust seismic inversion. *Entropy*, 22:464, 2020.
- [39] SL Da Silva, CA Da Costa, P Carvalho, J Araújo, L Lucena, and G Corso. An objective function based on  $q$ -gaussian distribution for full-waveform inversion. In *82nd EAGE Annual Conference & Exhibition*, volume 2020, pages 1–5. European Association of Geoscientists & Engineers, 2020.
- [40] João V. T. de Lima, Sérgio Luiz E. F. da Silva, João M. de Araújo, Gilberto Corso, and Gustavo Z. dos Santos Lima. Nonextensive statistical mechanics for robust physical parameter estimation: the role of entropic index. *Eur. Phys. J. Plus*, 136(3), March 2021.
- [41] S. L. E. F. da Silva, G. Z. dos Santos Lima, E. V. Volpe, and et al. Robust approaches for inverse problems based on Tsallis and Kaniadakis generalised statistics. *Eur. Phys. J. Plus*, 136:518, 2021.
- [42] Sérgio L. E. F. da Silva, J. Lopez, J. M. de Araújo, and G. Corso. Multi-scale  $q$ -FWI applied to circular shot OBN acquisition for accurate pre-salt velocity estimates. *IMAGE Technical Program Expanded Abstracts*, pages 712–716, 2021.
- [43] Jacques Hadamard. Sur les problèmes aux dérivés partielles et leur signification physique. *Princeton University Bull.*, 13:49–52, 1902.
- [44] Jon F. Claerbout and Francis Muir. Robust modeling with erratic data. *Geophysics*, 38(5):826–844, October 1973.
- [45] Alfréd Rényi et al. On measures of entropy and information. In *Proceedings of the Fourth Berkeley Symposium on Mathematical Statistics and Probability, Volume 1: Contributions to the Theory of Statistics*. The Regents of the University of California, 1961.
- [46] Shui-Hua Wang, Khan Muhammad, Yiding Lv, Yuxiu Sui, Liangxiu Han, and Yu-Dong Zhang. Identification of Alcoholism Based on Wavelet Renyi Entropy and Three-Segment Encoded Jaya Algorithm. *Complexity*, 2018:1–13, 2018.
- [47] P. Sánchez-Moreno, J.S. Dehesa, D. Manzano, and R.J. Yáñez. Spreading lengths of Hermite polynomials. *J. Comput. Appl. Math.*, 233(9):2136–2148, March 2010.
- [48] Xi Dong. The gravity dual of Rényi entropy. *Nat. Commun.*, 7(1):1–6, 2016.
- [49] Jose Costa, Alfred Hero, and Christophe Vignat. On solutions to multivariate maximum  $\alpha$ -entropy problems. In *International Workshop on Energy Minimization Methods in Computer Vision and Pattern Recognition*, pages 211–226. Springer, 2003.
- [50] O Johnson and C Vignat. Some results concerning maximum Rényi entropy distributions. *Ann. Inst. H. Poincaré B Probab. Stat.*, 43(3):339–351, May 2007.
- [51] S. Picoli Jr., R. S. Mendes, L. C. Malacarne, and R. P. B. Santos.  $q$ -distributions in complex systems: a brief review. *Braz. J. Phys.*, 39:468, 2009.
- [52] Sérgio Luiz Eduardo Ferreira da Silva. Newton’s cooling law in generalised statistical mechanics. *Physica A*, 565:125539, 2021.



- [53] Erick de la Barra and Pedro Vega-Jorquera. On q-pareto distribution: some properties and application to earthquakes. *Eur. Phys. J. B*, 94:32, 2021.
- [54] Sérgio Luiz Eduardo Ferreira da Silva and Gilberto Corso. Nonextensive Gutenberg-Richter law and the connection between earthquakes and marsquakes. *Eur. Phys. J. B*, 94:25, 2021.
- [55] H. Suyari and M. Tsukada. Law of Error in Tsallis Statistics. *IEEE Trans. Inf. Theory*, 51(2):753–757, February 2005.
- [56] C. Tsallis, R. S. Mendes, and A.R. Plastino. The role of constraints within generalized nonextensive statistics. *Physica A*, 261:534, 1998.
- [57] S. Abe and G. B. Bagci. Necessity of q-expectation value in nonextensive statistical mechanics. *Phys. Rev. E*, 71:016139, 2005.
- [58] Friedrich Schlögl. *Thermodynamics of chaotic systems: an introduction*. Cambridge University Press, 1993.
- [59] Sumiyoshi Abe. Remark on the Escort distribution representation of nonextensive statistical mechanics. *Phys. Lett. A*, 275(4):250–253, 2000.
- [60] Domingo Prato and Constantino Tsallis. Nonextensive foundation of Lévy distributions. *Phys. Rev. E*, 60(2):2398, 1999.
- [61] Yoshihiko Hasegawa and Masanori Arita. Properties of the maximum q-likelihood estimator for independent random variables. *Physica A*, 388(17):3399–3412, 2009.
- [62] G. Kaniadakis. Statistical mechanics in the context of special relativity. *Phys. Rev. E*, 66:056125, Nov 2002.
- [63] Giorgio Kaniadakis, Mauro M. Baldi, Thomas S. Deisboeck, Giulia Grisolia, Dionissios T. Hristopoulos, Antonio M. Scarfone, Amelia Sparavigna, Tatsuaki Wada, and Umberto Lucia. The  $\kappa$ -statistics approach to epidemiology. *Sci. Rep.*, 10:19949, 2020.
- [64] Sérgio Luiz E. F. da Silva.  $\kappa$ -generalised Gutenberg–Richter law and the self-similarity of earthquakes. *Chaos Solitons Fractals*, 143:110622, 2021.
- [65] Giorgio Kaniadakis. New power-law tailed distributions emerging in  $\kappa$ -statistics. *EPL*, 133:10002, 2021.
- [66] A.P. Santos, R. Silva, J.S. Alcaniz, and D.H.A.L. Anselmo. Kaniadakis statistics and the quantum h-theorem. *Phys. Lett. A*, 375(3):352–355, January 2011.
- [67] Sérgio Luiz E. F. da Silva, Gustavo Z. dos Santos Lima R. Silva, João M. de Araújo, and Gilberto Corso. An outlier-resistant  $\kappa$ -generalized approach for robust physical parameter estimation. *arXiv:2111.09921*, 2021.
- [68] Sanford Weisberg. *Applied linear regression*, volume 528. John Wiley & Sons, 2005.
- [69] Brian Russell and Dan Hampson. *Comparison of poststack seismic inversion methods*, page 876. SEG Technical Program Expanded Abstracts, 1991.
- [70] Mrinal K Sen. *Seismic inversion*. SPE, 2006.
- [71] Hao Wu, Shu Li, Yingpin Chen, and Zhenming Peng. Seismic impedance inversion using second-order overlapping group sparsity with A-ADMM. *J. Geophys. Eng.*, 17(1):97–116, 2020.
- [72] R. Versteeg. The Marmousi experience: Velocity model determination on a synthetic complex data set. *Lead. Edge*, 13:927–936, 1994.
- [73] G.S. Martin, R. Wiley, and K.J. Marfurt. Marmousi2: An elastic upgrade for Marmousi. *Lead. Edge*, 25:156–166, 2006.
- [74] N. Ricker. Further developments in the wavelet theory of seismogram structure. *Bull. Seismol. Soc. Am.*, 3:197–228, 1943.
- [75] N. Ricker. Wavelet functions and their polynomials. *Geophysics*, 9:314–323, 1944.
- [76] Eduard Stiefel. Methods of conjugate gradients for solving linear systems. *J. Res. Nat. Bur. Standards*, 49:409–435, 1952.
- [77] John Alan Scales, Martin Lloyd Smith, and Sven Treitel. *Introductory geophysical inverse theory*. Citeseer, 1994.
- [78] James D Evans. *Straightforward statistics for the behavioral sciences*. Thomson Brooks/Cole Publishing Co, 1996.